Attitude Correction for Oblate Earth

The horizon sensor output generates the chord width and phase through electronic detectors. As the conical horizon sensor spins, the detector electronics periodically sense rapid changes in IR intensity and produce pulses of incoming and outgoing scans. The time between these pulses (i.e., t_i and t_o), the sensor scanning speed ω, and the reference time t_r are used to compute the measured half-chord width and phase using

$$\Omega_{\text{meas}} = \omega(t_o - t_i)/2; \qquad \Delta_{\text{meas}} = \omega[(t_o - t_r) - (t_r - t_i)]/2 \quad (22)$$

Using these measured half-chord width and phase and assuming a spherical Earth, the flight software computes the roll and pitch estimates using Eq. (8) or (10). For the case of zero canting angle, the pitch estimate in Eq. (10) can be simplified even further to minimize the flight software computation. Define a reference half-chord width as Ω_{ref}. This reference chord is obtained by solving Eq. (10) with zero pitch. Then, a simplified pitch equation is

$$\theta = \tan(\alpha)\sin\{\cos^{-1}[\cos(\eta)/\sin(\alpha)]\}(\Omega_{\text{meas}} - \Omega_{\text{ref}}) \quad (23)$$

For oblateness corrections, Eqs. (10) and (24) can be modified as

$$\phi = \Delta_{\text{meas}} + \Delta_{\text{spher}} - \Delta_{\text{obl}} \quad (24)$$

$$\theta = K_\theta(\Omega_{\text{meas}} - \Omega_{\text{ref}} + \Omega_{\text{spher}} - \Omega_{\text{obl}}) \quad (25)$$

where

$$K_\theta = \tan(\alpha)\sin\{\cos^{-1}[\cos(\eta)/\sin(\alpha)]\} \quad (26)$$

Example

Given a sun synchronous satellite in a circular orbit with the orientation shown in Figs. 1 and 2, the orbit inclination is at 98.7 deg and the altitude is at 852 km; without loss of generality, the longitude of the ascending node λ and the canting angle γ are assumed zero. The scanning horizon sensor is mounted such that the center of the cone is along the negative X direction (i.e., direction opposite to spacecraft orbital velocity) and the half-cone angle is 60 deg. The transformation matrix from inertial to sensor coordinates is a function of the orbit phase σ and inclination angle i:

$$A_{s\leftarrow I} = \begin{bmatrix} 0 & 1 & 0 \\ 0 & 0 & -1 \\ -1 & 0 & 0 \end{bmatrix} \times \begin{bmatrix} \cos(\sigma) & \sin(\sigma) & 0 \\ -\sin(\sigma) & \sin(\sigma) & 0 \\ 0 & 0 & 1 \end{bmatrix} \begin{bmatrix} 1 & 0 & 0 \\ 0 & \cos(i) & \sin(i) \\ 0 & -\sin(i) & \cos(i) \end{bmatrix} \quad (27)$$

The horizon crossing vectors, $\boldsymbol{L}_i^I$ and $\boldsymbol{L}_o^I$, for both spherical and oblate Earth are computed using Eq. (21) and the Newton–Raphson algorithm. Figure 3 shows the oblateness errors for this condition. The errors are defined as the difference in the attitude as computed from spherical and oblate Earth models:

$$e_\phi = \phi_{\text{spher}} - \phi_{\text{obl}}; \qquad e_\theta = \theta_{\text{spher}} - \theta_{\text{obl}} \quad (28)$$

The observations are that the roll and pitch error magnitude can be as large as 0.05 and 0.5 deg, respectively, and are at the maximum when the sensor scans at around the polar regions. The error magnitude suggests that for stringent satellite pointing requirements, the sensor data corrections must be implemented.

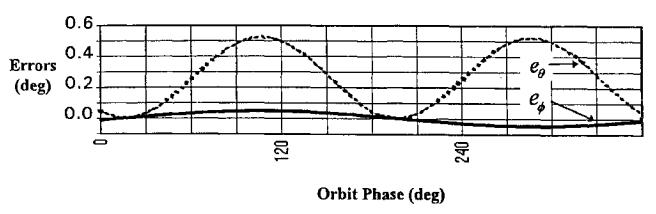

Fig. 3 Roll and pitch differences between spherical and oblate Earth models. Sun synchronous satellite with 98.7 deg inclination and 852 km altitude.

Conclusions

This Note has shown a simple method for estimating and correcting satellite roll and pitch attitude for single scanning horizon sensor configurations with the Earth oblateness effect. The study shows that the effect of Earth oblateness on the sensor measurements errors can be large for a LEO satellite. However, the attitude estimate errors because of oblateness can be reduced by including corrections in the flight software. Although the discussion has been concentrated on a single scanning type horizon sensor, the results are applicable to a wide variety of horizon sensor configurations.

Reference

[1]Wertz, J. R., *Spacecraft Attitude Determination and Control*, Kluwer Academic, Dordrecht, The Netherlands, 1978, pp. 98–106.

Detumbling and Reorienting Underactuated Rigid Spacecraft

Victoria Coverstone-Carroll*
University of Illinois at Urbana–Champaign, Urbana, Illinois 61801-2935

Introduction

UNDERACTUATED systems are dynamic systems that have more degrees of freedom (DOF) than number of actuators. Controlling all of the DOF in an underactuated system can present a challenging control problem; however, several benefits result if underactuated systems can be effectively controlled. First, control of these systems would allow some fully actuated systems (equal number of controller to DOF) to be operated as underactuated. Examples of this type include the control of a space-based robot. In this case the space-based robot possesses six DOF for the platform along with the n DOF associated with the n links of the robot. Normally, the platform is fully actuated with controllers for both translation and rotation; however, if actuators on the robot are used to reorient the platform, propellant can be conserved.[1,2] Also, even though underactuated systems are unconventional and more difficult to control, they have the advantage over fully actuated systems of being easier to design and cheaper to build. With the move toward smaller, faster to manufacture, and cheaper spacecraft, underactuated control has some distinct advantages. Finally, systems that suffer partial actuator failure might still be able to complete the objective of the original system.

Recently, researchers have developed control algorithms to detumble and reorient underactuated (active control around only two of the principal axes) spacecraft. Byrnes and Isidori[3] proved that a continuous feedback control law cannot asymptotically stabilize a rigid spacecraft with only two controls. Krishnan et al.[4] derived a discontinuous feedback control law that stabilized the spacecraft about any equilibrium attitude; however, a series of eight maneuvers is required. Also, Krishnan et al.[5] have considered stabilizing an underactuated rigid spacecraft using two momentum wheels with the assumption that the initial velocity vector lies in the same plane as the two momentum wheels. Tsiotras and Longuski[6] have considered

Received April 27, 1995; revision received Jan. 16, 1996; accepted for publication Jan. 20, 1996.

*Assistant Professor, Department of Aeronautical and Astronautical Engineering, 306 Talbot Laboratory, 104 S. Wright Street. Member AIAA.

stabilizing an axially symmetric spacecraft using only two external pairs of gas jets; however, the initial velocity vector is restricted to the control input plane. Here a variable structure controller is used to detumble the spacecraft. Once detumbled, linear feedback controllers can reorient the spacecraft to any orientation.

Problem Statement

For a rigid spacecraft, Euler's equations describe the relationship between an externally applied torque and the time rate of change of the angular velocity components ($\omega_1, \omega_2, \omega_3$) about the principal axes ($\boldsymbol{e}_1, \boldsymbol{e}_2, \boldsymbol{e}_3$) (Ref. 7):

$$\dot{\omega}_1 = -\lambda_1 \omega_2 \omega_3 \tag{1a}$$

$$\dot{\omega}_2 = -\lambda_2 \omega_1 \omega_3 + (\tau_2/I_2) \tag{1b}$$

$$\dot{\omega}_3 = -\lambda_3 \omega_1 \omega_2 + (\tau_3/I_3) \tag{1c}$$

Here $\lambda_1 = (I_3 - I_2)/I_1$, $\lambda_2 = (I_1 - I_3)/I_2$, and $\lambda_3 = (I_2 - I_1)/I_3$ and are assumed constant. Note that without loss of generality, principal axis 1 is defined as the passive axis, i.e., $\tau_1 = 0$. It is assumed that the spacecraft has at least one nonzero angular velocity component about an active axes ($\boldsymbol{e}_2$ or $\boldsymbol{e}_3$). If the only nonzero component of angular velocity that exists is about $\boldsymbol{e}_2$ or $\boldsymbol{e}_3$, a simple linear feedback controller can be designed to drive ω_2 or ω_3 to zero. If the only nonzero angular velocity is about $\boldsymbol{e}_1$, then to use the following analysis, a small angular component about $\boldsymbol{e}_2$ or $\boldsymbol{e}_3$ would need to be provided for dynamic coupling. Also, it is assumed that λ_1 is nonzero.

The control algorithm used to detumble the spacecraft is a variable structure controller (VSC). For a general treatment of VSC, see Ref. 8. Variable structure control requires the construction of a sliding surface. Here, the sliding surface is designed so that the angular velocity about the passive axis exponentially decays. This surface s, is represented as follows, where the constant k_1 is positive:

$$s = \dot{\omega}_1 + k_1 \omega_1 = -\lambda_1 \omega_2 \omega_3 + k_1 \omega_1 \tag{2}$$

The two torques (τ_2 and τ_3) are designed to drive the system to the surface ($s = 0$) and keep it there. Also, it is desirable to determine controllers such that once on the surface, all three angular velocity components exponentially decay. From Eq. (2), it is evident that the angular velocity about $\boldsymbol{e}_1$ exponentially decays, $\omega_1(t) = \omega_1(t_s)\exp[-k_1(t - t_s)]$ for $t_s \leq t$, after the surface has been reached.

The Lyapunov function $V(s) = s^2/2$ is used to design the control algorithms. Note that $V(s)$ is positive definite except when $s = 0$. The control algorithms are selected to force the derivative of $V(s)$ to be negative definite along the system trajectories described in Eq. (1); i.e., $V(s)$ is asymptotically decreasing in value with time. The torques τ_2 and τ_3 are chosen as described in Eqs. (3) and (4), which results in a negative definite Lyapunov function derivative until the sliding surface is reached, as shown in Eq. (5):

$$\tau_2 = I_2 \lambda_2 \omega_1 \omega_3 - k_2 I_2 \omega_2 + I_2 k_4 \,\mathrm{sat}(s\lambda_1 \omega_3, \varepsilon) \tag{3}$$

$$\tau_3 = I_3(k_2 - k_1)\omega_3 + I_3 \lambda_3 \omega_1 \omega_2 + I_3 k_3 \,\mathrm{sat}(s\lambda_1 \omega_2, \varepsilon) \tag{4}$$

$$\dot{V}(s) = -(s\lambda_1 \omega_2) k_3 \,\mathrm{sat}(s\lambda_1 \omega_2, \varepsilon) - (s\lambda_1 \omega_3) k_4 \,\mathrm{sat}(s\lambda_1 \omega_3, \varepsilon) \tag{5}$$

The saturation function that appears in the torque definitions is given in Eq. (6) and is introduced to minimize chattering in the controllers. A more thorough discussion of chattering control can be found in Ref. 8. The parameter ε is a small positive quantity, and the parameters k_3 and k_4 must be positive. The control laws just described may require torque magnitudes that span large ranges and, therefore, may be difficult to implement:

$$\mathrm{sat}(x, \varepsilon) = \begin{cases} \mathrm{sign}(x) & \text{for } |x| > \varepsilon \\ x/\varepsilon & \text{for } |x| \leq \varepsilon \end{cases} \tag{6}$$

Once the sliding surface has been reached ($s = 0$), Eqs. (3) and (4) simplify to continuous feedback control laws and are referred to as the equivalent torques:

$$\tau_{2_{\mathrm{eq}}} = I_2 \lambda_2 \omega_1 \omega_3 - k_2 I_2 \omega_2 \tag{7}$$

$$\tau_{3_{\mathrm{eq}}} = I_3(k_2 - k_1)\omega_3 + I_3 \lambda_3 \omega_1 \omega_2 \tag{8}$$

On the sliding surface, the given torques may be substituted into the second and third equations in Eq. (1) to yield linear angular velocity dynamics about $\boldsymbol{e}_2$ and $\boldsymbol{e}_3$:

$$\dot{\omega}_2 = -k_2 \omega_2 \tag{9}$$

$$\dot{\omega}_3 = (k_2 - k_1)\omega_3 \tag{10}$$

From Eq. (10), it is noticed that the parameter k_1 must be chosen larger than k_2 if ω_3 is to decrease with time. It is also important to have k_1 sufficiently larger than k_2 so that ω_1 decays to zero before either ω_2 or ω_3. Integrating Eqs. (9) and (10), with the assumption that $k_1 > k_2$, yields the desired exponential decay of ω_2 and ω_3 for $t_s \leq t$. Therefore, the control laws supplied through Eqs. (3) and (4) will guarantee exponential decay of all of the angular velocities once the sliding surface has been reached.

The torque generators (thrusters) may have a maximum torque magnitude that they can produce. If the algorithms in Eqs. (3) and (4) yield a torque that exceeds this magnitude, the torquers saturate. If this occurs, the applied torques have the same sign as the torques calculated in Eqs. (3) and (4), but the magnitude is set at the upper bound. The effect of torque saturation on the system is to slow the convergence to the sliding manifold; however, convergence is still maintained. This concept will be illustrated in the following example.

The attitude of a spacecraft can be parameterized in a variety of ways. Shuster[9] provides a survey of representations. A convenient parameterization of the spacecraft orientation is a sequence of three rotations about body-fixed axes, in particular, the active principal axes. Therefore, the 3-2-3 Euler set can be used where the integer sequence denotes the principal axis rotation sequence. After the spacecraft is at rest, simple linear controllers can be used for the single-axis reorientation maneuvers.

Spacecraft Detumbling Simulation

A detumbling maneuver for an underactuated spacecraft is simulated. The principal moments of inertia are assumed to be $I_1 = 90$, $I_2 = 105$, and $I_3 = 120$ kg-m^2. Initial angular velocities of $\omega_1(t_0) = 0.1$, $\omega_2(t_0) = -0.1$, and $\omega_3(t_0) = 0.1$ rad/s are imparted to the spacecraft. Three cases are discussed: no constraints on the available torque magnitude and a torque magnitude constraint of 5 and 2.5 Nm. The values of the parameters used in the simulations are $k_1 = 0.96$, $k_2 = 0.77$, $k_3 = 0.10$, and $k_4 = 0.08$. A genetic algorithm (GA) was used to select the gain values. A GA is an optimization search technique. The GA objective was to minimize the sum of the angular velocities at the final maneuver time. The small parameter ε is set at 0.0001.

The time required to reach the sliding surface depends on many parameters, maximum available torque being one. As the torque magnitude becomes more constrained, a delay in reaching the surface ($s = 0$) occurs. When no torque limits are imposed, the surface is reached in 17 s with the time increasing to 20 and 35 s as the constraint becomes more severe.

Figure 1 displays the angular velocity for the passive axis. Because of the initial positive $\dot{\omega}_1$, an initial increase in ω_1 is observed. The unconstrained maneuver drives the angular velocity to zero more quickly than the constrained cases; however, for all cases, exponential decay to zero begins when the system is close to the switching surfaces. Exponential decay of the angular velocities about the two active axes also begins when the switching surface is reached. Figure 2 displays the angular velocity about $\boldsymbol{e}_3$. The angular velocity decay rate ($k_1 - k_2$) is smaller than the other two axes decay rates. Comparing Figs. 1 and 2, it is also noted that the angular velocity about axis 1 decreases toward zero faster than

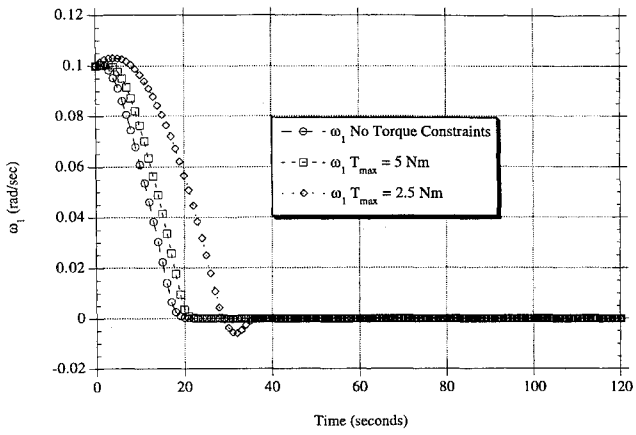

Fig. 1 Angular velocity about e_1 vs time.

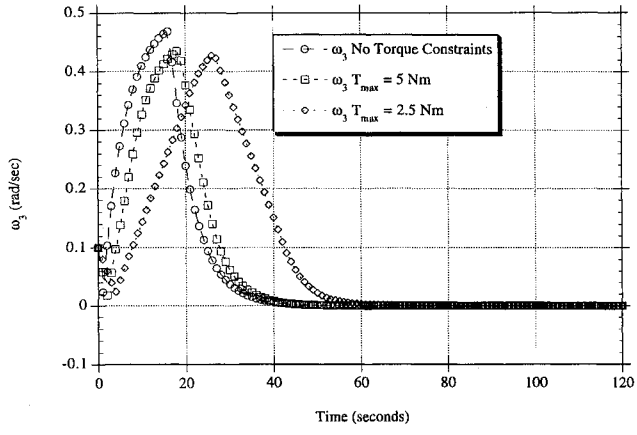

Fig. 2 Angular velocity about e_3 vs time.

the angular velocity about axis 3. A similar statement is true for the angular velocity about e_2, although a figure is not included for succinctness.

Conclusions

Underactuated spacecraft can be detumbled using a variable structure controller. The algorithm converges to a sliding surface on which exponential decay of the angular velocities occurs. Lower maximum torque magnitudes results in slower convergence to the sliding surface. Once the spacecraft is at rest, a series of at most three rotations about the two active axes is used to reorient the spacecraft. Simple linear controllers can be used for the reorientation maneuvers.

References

[1]Coverstone-Carroll, V., and Wilkey, N. M., "Optimal Control of a Satellite-Robot System Using Direct Collocation with Nonlinear Programming," *Acta Astronautica*, Vol. 36, No. 3, 1995, pp. 149–162.

[2]Mukherjee, R., and Chen, D., "Control of Free-Flying Underactuated Space Manipulators to Equilibrium Manifolds," *IEEE Transactions on Robotics and Automation*, Vol. 9, No. 5, 1993, pp. 561–569.

[3]Byrnes, C., and Isidori, A., "On the Attitude Stabilization of Rigid Spacecraft," *Automatica*, Vol. 27, No. 1, 1991, pp. 87–95.

[4]Krishnan, H., Reyhanoglu, M., and McClamroch, H., "Attitude Stabilization of a Rigid Spacecraft Using Two Control Torques: A Nonlinear Control Approach Based on the Spacecraft Attitude Dynamics," *Automatica*, Vol. 30, No. 6, 1994, pp. 1023–1027.

[5]Krishnan, H., McClamroch, N., and Reyhanoglu, M., "Attitude Stabilization of a Rigid Spacecraft Using Two Momentum Wheel Actuators," *Journal of Guidance, Control, and Dynamics*, Vol. 18, No. 2, 1995, pp. 256–263.

[6]Tsiotras, P., and Longuski, J. M., "On Attitude Stabilization of Symmetric Spacecraft with Two Control Torques," *Proceedings of the American Control Conference*, Vol. 1, American Automatic Control Council, San Francisco, CA, 1993, pp. 46–50.

[7]Kaplan, M., *Modern Spacecraft Dynamics and Control*, Wiley, New York, 1976, p. 50.

[8]Slotine, J.-J. E., and Li, W., *Applied Nonlinear Control*, Prentice–Hall, Englewood Cliffs, NJ, 1991, Chap. 7.

[9]Shuster, M., "A Survey of Attitude Representations," *Journal of the Astronautical Sciences*, Vol. 41, No. 4, 1993, pp. 439–517.

Modeling of the Planar Motion of a Flexible Structure

Michael S. Holmes,* A. Ray,† and David R. Mudgett‡
Pennsylvania State University,
University Park, Pennsylvania 16802-1412

Introduction

SLEWING and vibration control of flexible structures have received a considerable amount of attention in recent years. A common control objective is to translate and/or rotate a structure from an initial position to a more desirable final position. Unfortunately, since the structure is flexible, any movement will induce vibration. Thus, the control action should also attempt to suppress any vibrations.

One example of flexible structure control is the fine pointing of a space structure. Vibrations will cause error in the fine pointing and, if severe enough, could even damage the structure. Lim and Balas[1] investigate the fine pointing performance of the controls–structures interaction evolutionary model, which is a laboratory model of a large flexible spacecraft assembled at NASA Langley Research Center. They consider structured and unstructured modeling uncertainties and use μ synthesis to obtain a robust controller.[2]

The objective of the research reported here is to support the planning and fabrication of an experimental facility to study the dynamics of a flexible structure. This involves proposing and modeling the plant, performing computer simulations on the model, and finally building the structure in the laboratory. The ultimate goal is to synthesize a robust control law for the slewing maneuver of the flexible structure. The contribution of this Engineering Note is the derivation of a nonlinear, small-order model for a two-dimensional flexible structure.

Modeling of the Flexible Structure

Figure 1 shows the configuration of the laboratory flexible structure, which was originally proposed by Lim.[3] This structure consists of a rigid body, which undergoes frictionless planar motion in the reference X frame. The center of mass (denoted c.m. in Fig. 1) of the rigid body relative to the X frame is represented by the time-dependent variables $x_1(t)$ and $x_2(t)$. The χ frame of the rigid body has a time-dependent angular orientation $\theta(t)$ with respect to the X frame. A slender flexible beam is connected to the rigid body via a torsional spring at the point (0, c) in the rigid body's χ frame. The beam is free to vibrate only in the plane of the X frame so that the system as a whole can be treated as a two-dimensional problem. The deflection of the flexible beam is expressed in terms of its own local coordinates of the ζ frame. When the flexible beam is undeformed in the equilibrium position, it lies along the ζ_1 axis. Since the beam is rigidly connected to the top end of the spring and the shape of the beam is expressed by a smooth function of the local (ζ frame) coordinates, both the displacement and the slope of the beam are zero at the origin of the ζ frame. As the spring twists, the beam's ζ frame is rotated by an angle of $\phi(t)$ with respect to the rigid body's χ frame.

Received Dec. 13, 1994; revision received Dec. 14, 1995; accepted for publication Dec. 14, 1995.

*Graduate Student, Department of Electrical Engineering.
†Professor, Department of Mechanical Engineering. Associate Fellow AIAA.
‡Assistant Professor, Department of Electrical Engineering.